

# Generating quadrature squeezed light with combined optomechanical coupling

Kenan Qu and G. S. Agarwal

*Department of Physics, Oklahoma State University, Stillwater, OK - 74078, USA*

(Dated: December 7, 2024)

The recent demonstration of cooling of a macroscopic silicon nitride membrane based on dissipative coupling makes dissipatively coupled optomechanical systems as promising candidates for squeezing. We theoretically show that such a system in a cavity on resonance can yield good squeezing which is comparable to that produced by dispersive coupling. We also report the squeezing resulting from the combined effects of dispersive and dissipative couplings and thus the device can be operated in one regime or the other. We derive the maximal frequency and quadrature angles to observe squeezing for given optomechanical coupling strengths. We also discuss the effects of temperature on squeezing.

PACS numbers: 42.50.Wk, 07.10.Cm, 07.60.Ly, 42.50.Ct

## I. INTRODUCTION

The field of cavity optomechanics continues to register significant progress and a comprehensive review has recently appeared [1]. The important developments include cooling of the mirror to its ground state [2–4], mode splitting [5, 6], electromagnetically induced transparency (EIT) and its various applications [7–14]. More recently, strictly quantum effects like squeezing of the mirror [15–22] and the cavity field [23–33] as well as generation of entangled photon pairs [34–36] are receiving considerable attention. Ponderomotive squeezing of light [24–29] using a on resonance driving laser is one of the most promising way to generate squeezed light in cavity optomechanics. Safavi-Naeini *et al.* [25] fabricated a silicon microchip into a micromechanical cavity resonator and they observe fluctuation spectrum at a level  $4.5 \pm 0.2\%$  below the shot-noise limit despite the mechanical resonators highly excited thermal state ( $10^4$  phonons). Purdy *et al.* [26] placed a low-mass partially reflective membrane made of silicon nitride in the middle of an optical cavity and pushed the squeezing limit to 32% (1.7dB) by cooling the membrane to about 1mK. New ways of optical squeezing in optomechanical systems were also proposed. One example is using a double-cavity optomechanical system to generate two-mode squeezed light [30, 31]. The other example [32] is to generate quadrature squeezed light using the dissipative nature of the mechanical resonator in a single cavity driven by two different detuned lasers. As a closely related subject, Lehnert’s group reported the experimental realization of entanglement between cavity output photon-photon pairs [34] and entanglement between mechanical motion and microwave fields [35].

It should be noted that much of the work on cavity optomechanics uses the dispersive coupling. However, there are few studies for dissipative coupling [37–44]—the intrinsic cavity lifetime depends on the mechanical motion. The theoretical analysis of dissipative coupling in cavity optomechanics was reported by Elste *et al.* [37]. They pointed out that the system gives rise to remarkable quantum noise interference effect which leads to the Fano lineshape in the backaction force noise spectra. Ex-

perimentally, Li *et al.* [38] for the first time reported dissipative coupling in a cavity optomechanics system that comprises a microdisk and a vibrating nanomechanical beam waveguide. Based on such a setup, Huang and Agarwal [39] proposed a scheme to beat the Standard Quantum Limit (SQL) by irradiation of squeezed light into the cavity. Hammerer’s group [40, 41] concentrate on the dissipative coupling by placing an optomechanical membrane inside a Michelson-Sagnac interferometer. This scheme is advantageous in the sense that the dissipative coupling is not due to internal dissipation, but the output photons are detectable. Weiss *et al.* [42] presented a comprehensive study of dissipative coupling in both the weak and strong coupling limit, and they found the parameter regions for amplification of cooling as well as EIT and normal-mode splitting. Wu *et al.* [43] experimentally reported the application of torque sensing by using dissipative optomechanical coupling in a photonic crystal split-beam nanocavity. Very recently, Sawadsky *et al.* [45] demonstrated cooling starting from room temperature to 126mK based on the combined effect of dissipative and dispersive coupling. This is quite a remarkable development where the couplings can be changed adding flexibility to the operation. Encouraged by the significant cooling in this experiment, we examine the optical squeezing that can be produced in dissipative optomechanical interaction.

In this paper, we develop analytically the theory of Ponderomotive squeezing in cavity optomechanics with dissipative coupling. We show that the squeezing magnitudes with dissipative coupling are comparable to those achieved using dispersive coupling. This novel squeezing scheme broadens the scope of the quantum study of nonlinear interaction in optomechanics. Our proposal is based on the parameters reported in [45], however, it is not limited to this system and is applicable to any optomechanical systems that can provide combined interactions. This squeezing scheme works in the unresolved sideband regime, which has advantages in its easier system fabrication requirements. Moreover, this particular parameter regime makes it feasible for obtaining squeezed light with low frequency mechanical oscillators, although

thermal phonons are still an issue. We show that the system can generate 3dB squeezed field by using reasonable driving laser powers when the thermal phonon occupancy is as large as  $1.5 \times 10^5$  (bath temperature  $T = 1\text{K}$  correspondingly). The effect of higher bath temperature can be offset by increasing the driving laser power. As a by-product, our theory explains the new instability region for small pump laser red-detunings which was discovered in the experiment [45].

The structure of this paper is organized as follows: In Sec. II, we introduce the Hamiltonian of the optomechanical system with both dispersive and dissipative couplings, and find the input-output relation for the cavity field. In Sec. III, we provide the analysis of the squeezing effects under purely dissipative coupling. We compare it with the conventional dispersive squeezing and show that they both generate squeezed output with similar magnitudes but in different quadratures. In Sec. IV, we study the effects of the combined coupling on the squeezing and find the optimal quadrature angle for squeezing. We also study the effects of the mechanical mode at finite temperature. In Sec. V, we analyze the effective detuning of the driving laser due to the change of cavity resonance frequency, and then show its effect on the squeezing spectra. We present our conclusion in Sec. VI.

## II. MODEL

We consider a optomechanical system in which a mechanical oscillator (frequency  $\omega_m$ ) is coupled to an electromagnetic cavity. We model the cavity mode with annihilation operator  $a$  and the mechanical oscillator with displacement  $x$  and momentum  $p$ , or with dimensionless operators  $Q = x/x_{\text{ZPF}}$  and  $P = (\hbar x_{\text{ZPF}})p$  where  $x_{\text{ZPF}} = \sqrt{m\omega_m/\hbar}$  is the mechanical zero-point fluctuation. The mechanical displacements weakly modulate the cavity resonance frequency  $\omega_c(Q)$  and damping rate  $\kappa(Q)$ . We expand them to the linear order to get  $\omega_c(Q) \cong \omega_c - g_\omega Q$  and  $\kappa(Q) \cong \kappa - g_\kappa Q$ , where the dispersive coupling constant  $g_\omega = (\partial\omega_c/\partial Q)$  and the dissipative coupling constant  $g_\kappa = (\partial\kappa/\partial Q)$ . In the general cases, the dispersive coupling is larger than the dissipative coupling by a factor  $g_\omega/g_\kappa = \omega_c/\kappa \gg 1$ . However, by placing a micro-membrane inside a Michelson-Sagnac interferometer, studies showed that  $g_\kappa$  and  $g_\omega$  can be made of the same order.

When the optomechanical system is driven by a strong laser with frequency  $\omega_l$  and power  $\mathcal{P}$ , the Hamiltonian can be written, in the rotating frame, as

$$H = \hbar(\omega_c - \omega_l)a^\dagger a + \frac{1}{2}\hbar\omega_m(Q^2 + P^2) - \hbar g_\omega a^\dagger a Q + i\hbar\sqrt{2\kappa(Q)}[a^\dagger(\mathcal{E}_l + a_{\text{in}}) - H.c.], \quad (1)$$

where  $\mathcal{E}_l = \sqrt{\frac{\mathcal{P}}{\hbar\omega_l}}$  and  $a_{\text{in}}$  represents the input vacuum noise. To proceed, we linearize the Hamiltonian following the standard procedure by writing  $a = a_s + a_1$ ,  $P =$

$P_s + P_1$  and  $Q = Q_s + Q_1$ . The mean values of the steady-state can be calculated as

$$a_s = \frac{\sqrt{2\kappa_s}\mathcal{E}_l}{\kappa_s + i\Delta_s}, \quad Q_s = \left(\frac{g_\omega}{\omega_m} + \frac{\Delta_s g_\kappa}{\kappa_s \omega_m}\right)|a_s|^2, \quad (2)$$

and  $P_s = 0$ . Under the effect of driving laser, the mechanical oscillator displacement  $Q_s$  modulates the cavity resonance frequency and decay rate are both modulated. Hence we define  $\Delta_s = (\omega_c - g_\omega Q_s) - \omega_l$  as the driving laser detuning from the effective cavity resonance frequency; and we define  $\kappa_s = \kappa - g_\kappa Q_s$  as the effective cavity decay rate. Both  $\Delta_s$  and  $\kappa_s$  depend on the power of the driving laser. However, by tuning the driving laser frequency  $\omega_l$ , one can always make it on resonance with the effective cavity frequency, *i.e.*  $\Delta_s = 0$ . Under this condition, the effective cavity decay rate is determined by the quadratic equation  $\kappa_s^2 - \kappa\kappa_s + 2\mathcal{E}_l^2 g_\omega g_\kappa / \omega_m = 0$ . In the typical optomechanical systems, the term  $2\mathcal{E}_l^2 g_\omega g_\kappa / \omega_m$  is negligible comparing to  $\kappa$  and hence  $\kappa_s \cong \kappa$ . For example with the parameters reported in [45],  $2\mathcal{E}_l^2 g_\omega g_\kappa / \omega_m < \kappa/10^3$  when the driving power is below 10mW.

Then the linearized Hamiltonian takes the form  $H = H_0 + H_{\text{int}} + H_{\text{damp}}$  and

$$\begin{aligned} H_0 &= \hbar\Delta_s a_1^\dagger a_1 + \frac{1}{2}\hbar\omega_m(Q_1^2 + P_1^2), \\ H_{\text{int}} &= -\hbar\frac{G_\omega^* a_1 + G_\omega a_1^\dagger}{\sqrt{2}}Q_1 - \hbar G_\kappa \frac{a_1^\dagger - a_1}{\sqrt{2}i}Q_1, \\ H_{\text{damp}} &= -\hbar\sqrt{2\kappa_s}(a_1^\dagger a_{\text{in}} - a_{\text{in}}^\dagger a_1) - \hbar\frac{G_\kappa a_{\text{in}}^\dagger - G_\kappa^* a_{\text{in}}}{2\sqrt{\kappa_s}}Q_1, \end{aligned} \quad (3)$$

where  $G_{\omega,\kappa} = \sqrt{2}a_s g_{\omega,\kappa}$  is the driving field enhanced dispersive (dissipative) coupling constant. The form of the Hamiltonian (4) suggests that it is more intuitive to write the cavity field in terms of its quadratures:  $X = (a_1 + a_1^\dagger)/\sqrt{2}$ ,  $Y = (a_1 - a_1^\dagger)/(\sqrt{2}i)$ , and  $[X, Y] = i$ . In this paper, we are interested in generating squeezing light in the output field. Under the effect of dissipative coupling, the standard input-output relation

$$a_{\text{in}} + a_{\text{out}} = \sqrt{2\kappa_s}\left(1 + \frac{g_\kappa}{2\kappa_s}\right)a \approx \sqrt{2\kappa_s}a, \quad (4)$$

since  $g_\kappa \ll \kappa_s$ . This relation holds for the field quadrature  $X_{\text{in}} + X_{\text{out}} \approx \sqrt{2\kappa_s}X$ , and similarly for  $Y$ . Hereafter, we first focus on the on resonance driving scenario ( $\Delta_s = 0$ ) and then discuss the squeezing effect with detuned driving by relaxing this condition. When  $\Delta_s = 0$ , the coupling strength  $G_{\omega,\kappa}$  is real. The dynamics of the system can be described using the quantum Langevin equations

$$\frac{1}{\omega_m}\ddot{Q}_1 + \frac{\gamma_m}{\omega_m}\dot{Q}_1 + \omega_m Q_1 = G_\omega X + G_\kappa Y + \frac{G_\kappa}{\sqrt{2\kappa_s}}Y_{\text{in}} + \xi, \quad (5)$$

$$\dot{X} = -\kappa_s X - G_\kappa Q_1 + \sqrt{2\kappa_s}X_{\text{in}}, \quad (6)$$

$$\dot{Y} = -\kappa_s Y + G_\omega Q_1 + \sqrt{2\kappa_s}Y_{\text{in}}. \quad (7)$$

Here,  $\xi$  models the Brownian noise acting on the mechanical oscillator, and it obeys  $\langle \xi(t)\xi(t') \rangle = \gamma_m(2\bar{n}_{\text{th}} + 1)\delta(t - t')$ , where  $\bar{n}_{\text{th}}$  is the mean phonon occupation number. The correlations for the vacuum field are  $2\kappa_s \langle X_{\text{in}}(t)X_{\text{in}}(t') \rangle = 2\kappa_s \langle Y_{\text{in}}(t)Y_{\text{in}}(t') \rangle = \kappa_s \delta(t - t')$ . In the unresolved-sideband limit  $\kappa_s \gg \omega_m \gg \gamma_m$ , hence the vacuum noise dominate over the Brownian mechanical noise at low  $\bar{n}_{\text{th}}$ .

We illustrate the coupling relations of the quantum noises in the optomechanical system, in Fig. 1. The field

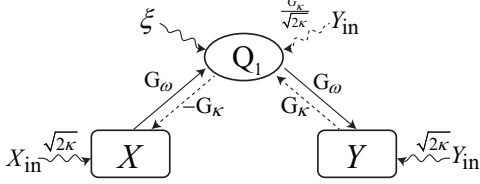


FIG. 1. The input quantum noises and their coupling relations among different quadratures ( $X$ ,  $Y$ ) of the cavity field and mechanical mode ( $Q_1$ ). The dashed arrows show the noise input and coupling due to dissipative coupling  $G_\kappa$ .

quadratures are subjected to the vacuum input noise  $X_{\text{in}}$  and  $Y_{\text{in}}$ . More importantly, we notice that, due to the dissipative coupling  $G_\kappa$ , the input vacuum noise  $Y_{\text{in}}$  is also coupled directly to the mechanical motion  $Q_1$ . At the same time, the form of the interaction Hamiltonian shows that  $Q_1$  interacts with the different cavity quadratures at the rates  $G_\omega$  and  $G_\kappa$ . Therefore,  $Y_{\text{in}}$  is fed into the system through two paths: (i) it directly couples to the cavity field; and (ii) it couples to the mechanical motion  $Q_1$  dissipatively then the optomechanical interaction transfer the noise to the cavity field. These two paths interfere in a coherent manner and lead to the Fano resonance in the cavity field spectrum.

We calculate the output field by combining Eqs.(4)-(7) after taking Fourier transform, and find

$$(\kappa_s - i\omega + \chi G_\omega G_\kappa)X_{\text{out}} + \chi G_\kappa^2 Y_{\text{out}} = (\kappa_s - \chi G_\omega G_\kappa)X_{\text{in}} - \sqrt{2\kappa_s} \chi G_\kappa \xi, \quad (8)$$

$$(\kappa_s - i\omega - \chi G_\omega G_\kappa)Y_{\text{out}} - \chi G_\omega^2 X_{\text{out}} = \chi G_\kappa^2 X_{\text{in}} + (\kappa_s + 2\chi G_\omega G_\kappa)Y_{\text{in}} - \sqrt{2\kappa_s} \chi G_\omega \xi, \quad (9)$$

where  $\chi = \omega_m/(\omega_m^2 - \omega^2 - i\omega\gamma_m)$  is the mechanical susceptibility. Eqs.(8) and (9) describes how the input quantum noises add to the quantum fluctuation of the output fields. Without optomechanical interactions, the output field preserves the input field fluctuations, *i.e.*,  $\langle X_{\text{out}}^2 \rangle = \langle Y_{\text{out}}^2 \rangle$ . As one increases the optomechanical interaction strengths  $G_\omega$  and  $G_\kappa$ , the noises are distributed in a nonlinear manner. The quantum squeezed states are generated when the variance is lower than the that of the coherent state, *i.e.*,  $S_\theta = \langle Z_\theta^2 \rangle < 1/2$  for a specific quadrature  $Z_{\theta\text{out}} = X_{\text{out}} \cos \theta + Y_{\text{out}} \sin \theta$ .

### III. SQUEEZING WITH PURELY DISSIPATIVE COUPLING

The phenomenon of Pondromotive squeezing with purely dissipative coupling can be obtained by setting the dispersive coupling strength  $G_\omega = 0$  and  $\Delta_s = 0$ , so that  $Y_{\text{out}} \cong (\chi G_\kappa^2/\kappa_s)X_{\text{in}} + Y_{\text{in}}$  and  $X_{\text{out}} + (\chi G_\kappa^2/\kappa_s)Y_{\text{out}} \cong X_{\text{in}}$  + mechanical noise. The vacuum input  $X_{\text{in}}$  is coupled, not only to  $X_{\text{out}}$ , but also to  $Y_{\text{out}}$  via the mediated mechanical mode  $Q_1$  scaled by the mechanical susceptibility  $\chi$  and dissipative coupling strength  $G_\kappa$ . When one measures the field  $Z_{\theta\text{out}} = X_{\text{out}} \cos \theta + Y_{\text{out}} \sin \theta$  at  $\theta \neq 0^\circ$  or  $90^\circ$ ,  $Y_{\text{out}}$  interferes partially with  $X_{\text{out}}$  since  $\chi(\omega)$  is generally complex. The interference leads to squeezed quantum noises. The output squeezing spectrum is

$$S_{\text{diss}} \cong \frac{1}{2} + \frac{G_\kappa^2}{\kappa_s} (2|\chi|^2 \Gamma_{\text{diss}} \cos^2 \theta - \text{Re} \chi \sin 2\theta), \quad (10)$$

where  $\Gamma_{\text{diss}} = G_\kappa^2/(4\kappa_s) + \gamma_m(2\bar{n}_{\text{th}} + 1)$  is the effective mechanical damping rate. By optimizing  $\theta$  and  $\chi(\omega)$  we obtain the optimal squeezing magnitude

$$S_{\text{diss}}^{\text{opt}} = \frac{\gamma_m(4\bar{n}_{\text{th}} + 3)}{G_\kappa^2/\kappa_s + 2\gamma_m(4\bar{n}_{\text{th}} + 3)}. \quad (11)$$

The squeezing magnitude can be enhanced by a large effective dissipative optomechanical coupling strength  $G_\kappa^2/(\kappa_s \gamma_m)$  and a low mean phonon occupancy number  $\bar{n}_{\text{th}}$ . The optimal squeezed quadrature angle lies at  $\tan \theta_{\text{diss}}^{\text{opt}} \cong -\sqrt{4G_\kappa^2/(\kappa_s \gamma_m)}$ , and  $\theta_{\text{diss}}^{\text{opt}}$  approaches to  $90^\circ$  with a large dissipative coupling strength  $G_\kappa$ . From the above analysis, we can see that the Pondromotive squeezing relies solely on the interference of two paths of  $X_{\text{in}}$ . One needs to suppress the input noises  $Y_{\text{in}}$  and  $\xi$  by choosing a quadrature angle  $\theta_{\text{diss}}^{\text{opt}}$  close to  $90^\circ$ . The output field shows anti-squeezing at  $\omega = \omega_m$  when  $\theta \neq 0$ . To illustrate the squeezing effect, we plot the output field spectra at different quadratures on Fig. 2(a) and (b) by numerically solving the quantum Langevin equations (5)-(7). We use the parameters provided by the experiment reported in [45], and the specific values are given in the caption of Fig. 2. At the angle  $\theta_{\text{diss}}^{\text{opt}}$ , the output spectrum (as shown in (b)) is characterized by a large squeezing of  $\sim 40\text{dB}$  at frequency  $\omega \sim \omega_m - 2\pi \times 15\text{Hz}$  and anti-squeezing at  $\omega = \omega_m$ .

In the other limit when dispersive coupling solely governs the optomechanical interaction, *i.e.*,  $G_\kappa = 0$ , Eqs. (8) and (9) reduce to  $X_{\text{out}} \cong X_{\text{in}}$  and  $Y_{\text{out}} \cong Y_{\text{in}} + (\chi G_\omega^2/\kappa_s)X_{\text{in}}$  + mechanical noise. This is the conventional Pondromotive squeezing scheme. It shares the similar noise transformation with which we discussed above. Hence we are able to observe similar squeezing phenomenon, but the optimal squeezed quadrature is around  $\tan \theta_{\text{disp}}^{\text{opt}} \cong \sqrt{\kappa_s \gamma_m/(2G_\omega^2)}$ , and  $\theta_{\text{disp}}^{\text{opt}}$  approaches to 0 with a large dispersive coupling strength  $G_\omega$ . The output squeezing spectrum is

$$S_{\text{disp}} \cong \frac{1}{2} + \frac{G_\omega^2}{\kappa_s} (2|\chi|^2 \Gamma_{\text{disp}} \sin^2 \theta + 2\text{Re} \chi \sin 2\theta), \quad (12)$$

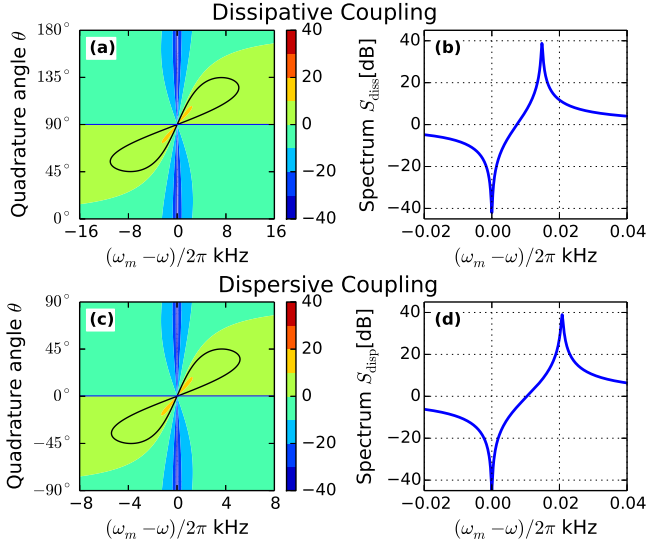


FIG. 2. Comparison of squeezing spectra with purely dissipative coupling [(a) and (b)] and purely dispersive coupling [(c) and (d)]: The regions inside the black contours in the density plots (a) and (c) show 3dB squeezing region and the blue horizontal lines show the optimal quadrature which are plotted in (b) and (d), correspondingly. The dissipative coupling strength is  $G_\kappa = 2\pi \times 150\text{kHz}$  with driving laser power  $\mathcal{P} \sim 3.5\text{W}$ ; the dispersive coupling strength is  $G_\omega = 2\pi \times 75\text{kHz}$  with driving laser power  $\mathcal{P} \sim 40\text{mW}$ . Other parameters are  $\kappa_s = 2\pi \times 1.5\text{MHz}$ ,  $\omega_m = 2\pi \times 136\text{kHz}$ ,  $\gamma_m = 2\pi \times 0.23\text{Hz}$ ,  $\Delta_s = 0$  and  $\bar{n}_{\text{th}} = 0$ .

where  $\Gamma_{\text{disp}} = G_\omega^2/\kappa_s + \gamma_m(2\bar{n}_{\text{th}} + 1)$ . By optimizing  $\theta$  and  $\chi(\omega)$  we obtain the optimal squeezing magnitude

$$S_{\text{disp}}^{\text{opt}} = \frac{\gamma_m(\bar{n}_{\text{th}} + 1)}{G_\omega^2/\kappa_s + 2\gamma_m(\bar{n}_{\text{th}} + 1)}. \quad (13)$$

This result is identical to the one derived in [27] and has been experimentally demonstrated in [25, 26]. The optimal output frequency is  $(\omega - \omega_m)^2 = \Gamma_{\text{disp}}\gamma_m/2 + \gamma_m^2/4$ , which increases with coupling strength  $G_\omega^2$ . We plot the output spectra of dispersive squeezing in Fig. 2(c) and (d), in comparison with the dissipative squeezing in (a) and (b). The optimal squeezing spectrum has a quadrature angle close to 0. The optimal squeezing magnitude is shown as  $\sim 30\text{dB}$ , which agrees with Eq. (13). We observe similar output squeezed spectra, although the optimal squeezing magnitude is smaller than (a) and (b) due to lower coupling strengths.

Physically both the dispersive coupling and the dissipative coupling generate optical squeezing in a similar manner, in the sense that they couple the input noise from one quadrature to the other quadrature coherently. Thus the input vacuum noise couples to the optomechanical system via two paths, as shown in Fig. 1. These two paths interfere and lead to squeezing. The optimal squeezing exists in different quadrature angles due to the fact that  $G_\omega$  couples noise from  $X$  to  $Y$  and  $G_\kappa$  couples noise from  $Y$  to  $X$  via the mechanical mode.

#### IV. SQUEEZING WITH COMBINED EFFECTS OF DISSIPATIVE AND DISPERSIVE COUPLING

In the previous section, we studied the squeezing phenomena with purely dispersive coupling or dissipative coupling. One natural question is if the combined effect of these two coupling regimes could enhance the squeezing. We next study the generation of squeezed state in present of both coupling regimes  $G_\omega$  and  $G_\kappa$ . When the driving laser frequency is on resonance  $\Delta_s = 0$ , according to Eq.(8), the input vacuum fluctuations destructively interfere when  $G_\omega G_\kappa \rightarrow \kappa_s/\chi$ . Complete destructive interference exists only when  $\chi$  is purely real, *i.e.*,  $\omega \gg \omega_m$ . The output squeezing spectrum is

$$S_{\text{disp}} \cong \frac{1}{2} + \frac{(G_\kappa \cos \theta - G_\omega \sin \theta)^2}{\kappa_s} \times [2|\chi|^2 \Gamma_{\text{comb}} - \text{Re}\chi \left( \frac{2G_\omega \cos \theta - G_\kappa \sin \theta}{G_\kappa \cos \theta - G_\omega \sin \theta} \right)], \quad (14)$$

where  $\Gamma_{\text{comb}} = (4G_\omega^2 + G_\kappa^2)/(4\kappa_s) + \gamma_m(2\bar{n}_{\text{th}} + 1)$ . The optimal squeezing quadrature angle  $\tan \theta_{\text{hybr}}^{\text{opt}} \sim G_\kappa/(2G_\omega)$  and the squeezing magnitude

$$S_{\text{comb}}^{\text{opt}} \cong \frac{1}{2} \cdot \frac{\gamma_m(2\bar{n}_{\text{th}} + 1)}{(G_\omega^2 + G_\kappa^2/4)/\kappa_s + \gamma_m(2\bar{n}_{\text{th}} + 1)}. \quad (15)$$

We see that the squeezing magnitude can be enhanced by increasing the coupling strengths  $G_\omega$  and  $G_\kappa$  for any given mean phonon number  $\bar{n}_{\text{th}}$ . The squeezed quadrature rotates from quadrature  $X$  to quadrature  $Y$  as the ratio of the coupling strengths  $G_\kappa/(2G_\omega)$  increases.

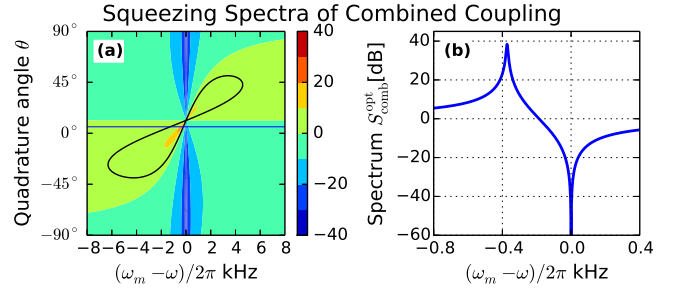


FIG. 3. The density plots (a) and the optimal squeezing quadrature (b) of the output field spectra with combined dispersive and dissipative couplings. The regions inside the black contours in (a) show 3dB squeezing region and the blue horizontal line shows the optimal quadrature which are plotted in (b). The coupling strengths are  $G_\omega = 2\pi \times 75\text{kHz}$  and  $G_\kappa = 2\pi \times 15\text{kHz}$  with driving laser power  $\mathcal{P} \sim 40\text{mW}$ . Other parameters are identical to those used in Fig. 2.

In Fig. 3(a), we plot the output spectra at different quadratures when the optomechanical system is subject to both dispersive and dissipative couplings. We set the coupling strengths such that  $G_\omega = 5G_\kappa$  in accordance with the experiment parameters in [45]. The density plot resembles the main feature of Poundrotative squeezing

with purely  $G_\omega$  or  $G_\kappa$ , except for a trivial quadrature difference. However, there are distinctions. The frequency bandwidth of the squeezing spectra increases in the large quadrature angle and shrinks in the lower quadrature angle. This is particularly advantageous in practise, since one usually focuses on a specific quadrature and hence one can make use of the larger bandwidth of the squeezed spectra.

In the optomechanical pondromotive squeezing process, the mechanical element functions as an active mediating element and it provides the coherent coupling between two field quadratures. At the same time, it is subject to the environment Brownian noise which is incoherent with the cavity field. In the reported Pondromotive squeezing experiments with purely dispersive optomechanical coupling, the environment temperature sets the limit of the squeezing magnitudes: Safavi-Naeini *et al.* [25] reported 0.2dB squeezing at  $\bar{n}_{\text{th}} \sim 10^4$  and Purdy *et al.* [26] pushed the squeezing magnitude to 1.7dB with a lower thermal phonon occupancy  $\bar{n}_{\text{th}} = 47$ .

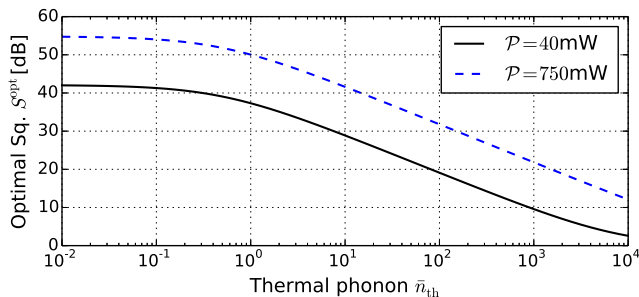


FIG. 4. The effects of the mean thermal phonon occupation  $\bar{n}_{\text{th}}$  on the optimal squeezing magnitudes with different couplings. The optimal squeezing magnitudes are very similar for finite  $\bar{n}_{\text{th}}$  hence the three curves overlap.

We now compare the effect of the thermal phonons on squeezing with with different optomechanical couplings. Eqs. (11), (13) and (15) indicate that the output quadrature variance increases approximately proportional to  $\bar{n}_{\text{th}}$  at large coupling rates. Comparing Eqs. (11) and (13), we find that optomechanical systems with purely dissipative coupling ( $G_\kappa$ ) or purely dispersive coupling ( $G_\omega$ ) can generate squeezed field of similar squeezing magnitude if  $G_\kappa = 2G_\omega$ . In Fig. 4(a), we illustrate the effects of the mean thermal phonon number on the optimal squeezing magnitude under different coupling regimes. The curves show that the squeezing magnitudes decreases with large thermal phonon occupancy  $\bar{n}_{\text{th}}$ . Even when the thermal phonon number is as high as  $\bar{n}_{\text{th}} = 1000$ , the system yields about 10dB squeezing with combination optomechanical couplings at  $\mathcal{P} = 40\text{mW}$ . If we increase the driving laser power to  $\mathcal{P} = 150\text{mW}$ , the squeezing magnitude increases to 15dB. Note that, this phonon number is however difficult to achieve with low mechanical frequency  $\omega_m$  since  $\bar{n}_{\text{th}}$  is inversely proportional to  $\omega_m$ . For exam-

ple, the system has to be pre-cooled down to  $T \sim 6.5\text{mK}$  in order to get  $\bar{n}_{\text{th}} = 1000$ . On the other hand at high bath temperature, large squeezing magnitude requires to increase the coupling strength, which can be achieved by increasing the pump power. If the bath temperature increases to  $T = 1\text{K}$ , the corresponding thermal phonon number increases to  $\bar{n}_{\text{th}} \sim 1.5 \times 10^5$ . One needs to increase the driving laser power to  $\mathcal{P} \sim 750\text{mW}$  in order to get 3dB squeezing.

## V. SQUEEZING WITH A FIXED FREQUENCY DRIVING LASER

Sawadsky *et al.* [45] demonstrated strong cooling effect in an optomechanical system with both dissipative and dispersive coupling interactions. The experimental results agree remarkably well with the theoretical calculation. In the experiment, the authors fix the driving laser frequency  $\omega_l$  on resonance with the empty cavity resonance frequency  $\omega_c$ . When the driving laser power in-

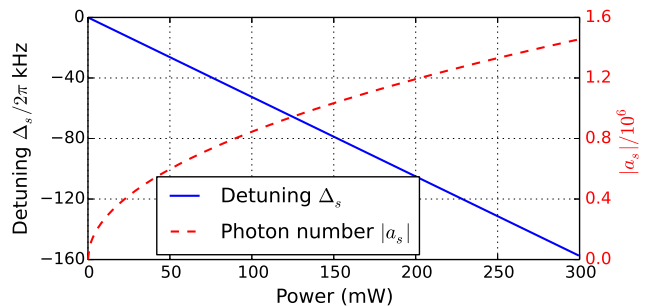


FIG. 5. The change of the effective detuning and mean cavity photon number as the driving laser power increases from 0 to 200mW. Other parameters are identical to those used in Figs. 3.

creases, the effective cavity resonance frequency changes due to the displacement of the mechanical membrane and this leads to an effective detuning of the driving laser. In this section, we analyze the squeezing phenomena in the optomechanical system driven by a laser with fixed frequency  $\omega_l = \omega_c$ . Under this condition, the effective detuning  $\Delta_s$  and effective cavity decay rate  $\kappa_s$  can be determined by solving the nonlinear equation set (2). We use the parameters reported in [45]. The solution to (2) shows that  $\kappa_s \sim \kappa$  when the driving laser power  $\mathcal{E}_l$  is below 250mW. However, the effective driving laser detuning  $\Delta_s$  increases linearly from 0 to a value close to  $-\omega_m$ , as shown in Fig. 5. The cavity mean photon number  $|a_s|$  is also displayed in Fig. 5. When the driving laser power is set as 40mW, the effective detuning  $\Delta_s = 2\pi \times 20\text{kHz}$ . The corresponding coupling strengths remain the values  $G_\omega = 2\pi \times 75\text{kHz}$ , which are similar to the ones used in Figs. 2 and 3. We show the squeezing spectra with different coupling interactions in Fig. 6 at zero temperature. Their optimal squeezing magnitudes reach close to

40dB. We find large regions with over 3dB squeezing in both spectra, as illustrated between the thick black 3dB contour lines. We observe large regions of squeezing over 10dB and in Fig. 6(b) even squeezing over 20dB. The results are very similar to the ones in Figs. 2(a) and 3(a), and even the effects of temperature are similar so they are not discussed here.

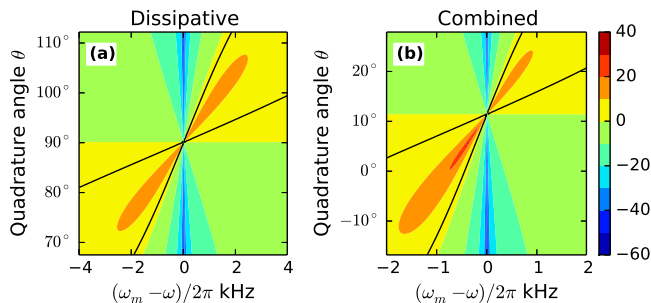


FIG. 6. The squeezing spectra in an optomechanical system with (a) purely dissipative coupling  $G_\kappa = 2\pi \times 150\text{kHz}$  and  $\mathcal{P} \sim 3.5\text{W}$ , and (b) combined both couplings with  $G_\omega = 5G_\kappa = 2\pi \times 75\text{kHz}$  and  $\mathcal{P} \sim 40\text{mW}$ . Other parameters are identical to those used in Figs. 2 or 3. The regions between the black contours have over 3dB squeezing.

## VI. CONCLUSION

In conclusion, we investigated the generation of quadrature squeezed states with dissipative coupling optomechanical interaction. Our results show that dissipative coupling interaction is able generate strong squeezed vacuum states. The squeezing magnitude depends on the coupling strengths and the mean phonon occupancy due to the mechanical noise. When the dissipative and dispersive coupling strengths are similar, they both generate comparable squeezing magnitude. This novel scheme works in the unresolved sideband limit which enables its application in low frequency mechanical oscillators. In potential experimental realizations, one challenge would be the large thermal noise introduced by the large phonon number with low mechanical frequency. Large squeezing magnitudes require one to pre-cool the system using a dilution refrigerator. The large thermal noise can also be offset by increasing the pump power by the same order of magnitude with  $\bar{n}_{\text{th}}$ .

## APPENDIX: STABILITY CRITERION

While we follow the standard linearization procedure in solving the nonlinear Hamiltonian, we must make sure the stability of the system dynamics for our chosen parameters. We investigate the dynamics of the system using the quantum Langevin equation

$$d\Psi(t)/dt = \mathbb{M}\Psi(t) + \Psi_{\text{in}}(t), \quad (16)$$

with  $\Psi(t) = (X, Y, Q_1, P_1)^T$  for the system operators,  $\Psi_{\text{in}}(t) = (\sqrt{2\kappa_s}X_{\text{in}}, \sqrt{2\kappa_s}Y_{\text{in}}, -\frac{\text{Im}G_\omega}{\sqrt{2\kappa_s}}X_{\text{in}}, \xi - \frac{\text{Re}G_\omega}{\sqrt{2\kappa_s}}Y_{\text{in}})^T$  for the input noises, and

$$\mathbb{M} = \begin{pmatrix} -\kappa_s & \Delta_s & -\text{Re}G_\omega - \text{Im}G_\omega & 0 \\ -\Delta_s & -\kappa_s & \text{Re}G_\omega & 0 \\ 0 & 0 & 0 & \omega_m \\ \text{Re}G_\omega & \text{Re}G_\omega + \text{Im}G_\omega & -\omega_m & -\gamma_m \end{pmatrix}. \quad (17)$$

The system is stable if all the eigenvalues of the matrix  $\mathbb{M}$  all have negative real parts. Before we present the stability condition using the Routh-Hurwitz criterion, we would like to make the following approximation. When the driving laser frequency is not far off-resonance ( $\Delta_s \sim 0$ ), the steady state of the field  $a_s \cong \sqrt{\frac{2}{\kappa_s}}\mathcal{E}_l(1 - i\frac{\Delta_s}{\kappa_s})$ . Note that although  $G_{\omega,\kappa}$  is generally complex, the imaginary part is smaller than the real part by a factor of  $\Delta_s/\kappa_s$ . In this paper, since we concentrate on the unresolved sideband limit regime,  $\kappa_s \gg \omega_m > \Delta_s$ , we can make the approximation  $(\text{Re}G_{\omega,\kappa})^2 \cong G_{\omega,\kappa}^2$  at a good precision. We find the condition for stability in our system

$$\Delta_s(G_\omega^2 + G_\kappa^2) - \omega_m(\kappa_s^2 + \Delta_s^2) < 0, \quad (18)$$

$$\frac{\omega_m \Delta_s}{2\kappa_s \gamma_m} (G_\omega^2 + G_\kappa^2) + \omega_m^2 + \left(\frac{\kappa_s^2 + \Delta_s^2 - \omega_m^2}{2\kappa_s + \gamma_m} + \frac{\gamma_m}{2}\right)^2 - \left(\frac{\gamma_m}{2}\right)^2 > 0. \quad (19)$$

Note that when  $G_\kappa \rightarrow 0$ , these conditions reduces to the stability condition for the optomechanical system with purely dispersive coupling  $G_\omega$ . In the unresolved sideband limit that  $\kappa_s \gg \omega_m \gg \gamma_m$ ,  $G_{\omega,\kappa}$  can be treated purely real and the conditions (18)-(19) are simplified as

$$-\frac{\gamma_m}{2\kappa_s \omega_m} (\kappa_s^2 + \Delta_s^2)^2 < \Delta_s(G_\omega^2 + G_\kappa^2) < \omega_m(\kappa_s^2 + \Delta_s^2). \quad (20)$$

From the condition, one can see the system is always stable when  $\Delta_s = 0$ . For small negative  $\Delta_s$ , the first inequality in (20) imposes a very tight condition on the stability. Especially with a very high mechanical quality factor  $Q = \omega_m/\gamma_m$ , the condition reduces to  $(|2\Delta_s/\kappa_s|)(G_\omega^2 + G_\kappa^2)/\kappa_s^2 < 1/Q$ . This explains the instability region discovered in [45].

- 
- [1] M. Aspelmeyer, T. J. Kippenberg, and F. Marquardt, *Rev. Mod. Phys.* **86** (2014). See also C. Genes, A. Mari, D. Vitali, and P. Tombesi, *Adv. At. Mol. Opt. Phys.*, **57**, 33 (2009), Y. Chen, *J. Phys. B* **46**, 104001 (2013); and P. Meystre, *Ann. Phys. (Berlin)* **525**, 215 (2013).
- [2] I. Wilson-Rae, N. Nooshi, W. Zwerger, and T. J. Kippenberg, *Phys. Rev. Lett.* **99**, 093901 (2007).
- [3] F. Marquardt, J. P. Chen, A. A. Clerk, and S. M. Girvin, *Phys. Rev. Lett.* **99**, 093902 (2007).
- [4] J. D. Teufel, *et al.*, *Nature (London)* **475**, 359 (2011).
- [5] J. M. Dobrindt, I. Wilson-Rae, and T. J. Kippenberg, *Phys. Rev. Lett.* **101**, 263602 (2008).
- [6] S. Groeblacher, K. Hammerer, M. R. Vanner and M. Aspelmeyer, *Nature* **460**, 724 (2009).
- [7] G. S. Agarwal and S. Huang, *Phys. Rev. A* **81**, 041803(R) (2010).
- [8] S. Weis, *et al.*, *Science* **330**, 1520 (2010); J. D. Teufel, *et al.*, *Nature (London)*, **471**, 204 (2011).
- [9] Y. Liu, M. Davanço, V. Aksyuk, and K. Srinivasan, *Phys. Rev. Lett.* **110**, 223603 (2013).
- [10] J. Kim, M. Kuzyk, K. Han, H. Wang, and G. Bahl, *Nature Phys.*, **11**, 275 (2015).
- [11] C. Dong, Z. Shen, C. Zou, Y. Zhang, W. Fu, and G. Guo, *Nature Commun.* **6**, 6193 (2015).
- [12] Kenan Qu and G. S. Agarwal, *Phys. Rev. A* **87**, 031802 (2013).
- [13] A. H. Safavi-Naeini, *et al.*, *Nature (London)*, **472**, 69 (2011).
- [14] V. Fiore, Y. Yang, M. C. Kuzyk, R. Barbour, L. Tian, and H. Wang, *Phys. Rev. Lett.* **107**, 133601 (2011).
- [15] A. Heidmann, Y. Hadjar, and M. Pinard, *Appl. Phys. B* **64**, 173 (1997).
- [16] K. Jähne, C. Genes, K. Hammerer, M. Wallquist, E. S. Polzik, P. Zoller, *Phys. Rev. A* **79**, 063819 (2009).
- [17] X.-Y. Lü, J.-Q. Liao, L. Tian, and F. Nori, *Phys. Rev. A* **91**, 013834 (2015).
- [18] P. Rabl, A. Shnirman, and P. Zoller, *Phys. Rev. B* **70**, 205304 (2004).
- [19] E. A. Sete and H. Eleuch, *Phys. Rev. A* **89**, 013841 (2014).
- [20] J.-Q. Liao and C. K. Law, *Phys. Rev. A* **83**, 033820 (2011).
- [21] H. Tan, G. Li, and P. Meystre, *Phys. Rev. A* **87**, 033829 (2013).
- [22] A. Szorkovszky, A. C. Doherty, G. I. Harris, and W. P. Bowen, *Phys. Rev. Lett.* **107**, 213603 (2011).
- [23] M. Asjad, G. S. Agarwal, M. S. Kim, P. Tombesi, G. Di Giuseppe, and D. Vitali, *Phys. Rev. A* **89**, 023849 (2014).
- [24] A. Pontin, C. Biancofiore, E. Serra, A. Borrielli, F. S. Cataliotti, F. Marino, G. A. Prodi, M. Bonaldi, F. Marin, and D. Vitali, *Phys. Rev. A* **89**, 033810 (2014).
- [25] A. H. Safavi-Naeini, S. Gröblacher, J. T. Hill, J. Chan, M. Aspelmeyer, and O. Painter, *Nature (London)* **500**, 185 (2013).
- [26] T. P. Purdy, P.-L. Yu, R. W. Peterson, N. S. Kampel, and C. A. Regal, *Phys. Rev. X* **3**, 031012 (2013).
- [27] C. Fabre, M. Pinard, S. Bourzeix, A. Heidmann, E. Giacobino, and S. Reynaud, *Phys. Rev. A* **49**, 1337 (1994).
- [28] F. Marino, F. S. Cataliotti, A. Farsi, M. S. de Cumis, and F. Marin, *Phys. Rev. Lett.* **104**, 073601 (2010).
- [29] D. W. C. Brooks, T. Botter, S. Schreppler, T. P. Purdy, N. Brahms, and D. M. Stamper-Kurn, *Nature (London)* **448**, 476 (2012).
- [30] K. Qu, and G. S. Agarwal, *New J. Phys.*, **16**, 113004 (2014).
- [31] M. J. Woolley and A. A. Clerk, *Phys. Rev. A*, **89**, 063805 (2014).
- [32] A. Kronwald, F. Marquardt, and A. A. Clerk, *New J. Phys.*, **16**, 063058 (2014).
- [33] A. A. Clerk, F. Marquardt, and K. Jacobs, *New J. Phys.* **10**, 095010 (2008).
- [34] D. Ristè, M. Dukalski, C. A. Watson, G. de Lange, M. J. Tiggelman, Ya. M. Blanter, K. W. Lehnert, R. N. Schouten, L. DiCarlo, *Nature* **502**, 350 (2013).
- [35] T. A. Palomaki, J. D. Teufel, R. W. Simmonds, K. W. Lehnert, *Science* **342**, 710-713 (2013).
- [36] Y.-D. Wang and A. A. Clerk, *Phys. Rev. Lett.* **110**, 253601 (2013); L. Tian, *Phys. Rev. Lett.* **110**, 233602 (2013); Z.-Q. Yin, and Y.-J. Han, *Phys. Rev. A* **79**, 024301 (2009); M. C. Kuzyk, S. J. van Enk, and H. Wang, *Phys. Rev. A* **88**, 062341 (2013); C. Joshi, J. Larson, M. Jonson, E. Andersson, and P. Öhberg, *Phys. Rev. A* **85**, 033805 (2012).
- [37] F. Elste, S. M. Girvin, and A. A. Clerk, *Phys. Rev. Lett.*, **102**, 207209 (2009).
- [38] M. Li, W. H. P. Pernice, and H. X. Tang, *Phys. Rev. Lett.* **103**, 223901 (2009).
- [39] S. Huang and G. S. Agarwal, *Phys. Rev. A* **82**, 033811 (2010).
- [40] A. Xuereb, R. Schnabel, and K. Hammerer, *Phys. Rev. Lett.* **107**, 213604 (2011).
- [41] S. P. Tarabrin, H. Kaufer, F. Y. Khalili, R. Schnabel, and K. Hammerer, *Phys. Rev. A* **88**, 023809 (2013).
- [42] T. Weiss, C. Bruder, and A. Nunnenkamp, *New J. Phys.* **15**, 045017 (2013).
- [43] M. Wu, A. C. Hryciw, C. Healey, D. P. Lake, H. Jayakumar, M. R. Freeman, J. P. Davis, and P. E. Barclay, *Phys. Rev. X* **4**, 021052 (2014).
- [44] O. Kyriienko, T. C. H. Liew, and I. A. Shelykh, *Phys. Rev. Lett.* **112**, 076402 (2014).
- [45] A. Sawadsky, H. Kaufer, R. M. Nia, S. P. Tarabrin, F. Ya. Khalili, K. Hammerer, and R. Schnabel, *Phys. Rev. Lett.*, **114**, 043601 (2015).
- [46] A. A. Clerk, F. Marquardt, and K. Jacobs, *New J. Phys.*, **10**, 095010 (2008).
- [47] A. Szorkovszky, A. C. Doherty, G. I. Harris, and W. P. Bowen, *Phys. Rev. Lett.*, **107**, 213603 (2011).
- [48] A. Szorkovszky, G. A. Brawley, A. C. Doherty, and W. P. Bowen, *Phys. Rev. Lett.*, **110**, 184301 (2013).
- [49] M. Poot, K. Y. Fong, and H. X. Tang, *Phys. Rev. A* **90**, 063809 (2014).
- [50] M. Paternostro, S. Gigan, M. S. Kim, F. Blaser, H. Bhm, and M. Aspelmeyer, *New J. Phys.* **8**, 107 (2006).
- [51] A. Hurwitz, On the conditions under which an equation has only roots with negative real parts. *Selected Papers on Mathematical Trends in Control Theory.* (Dover, New York, 1964).